

Structural and magnetic properties of Co₂MnSi thin films

M. Belmeguenai^{1*}, F. Zighem², D. Faurie¹, S. M. Chérif¹, P. Moch¹, K. Westerholt³ and W. Seiler⁴

¹ LPMTM, Institut Galilée, UPR 9001 CNRS, Université Paris 13,
99 Avenue Jean-Baptiste Clément 93430 Villetaneuse, France

² IMCN, Université Catholique de Louvain, Place Croix du Sud 1, 1348 LLN, Belgium

³ *Experimentalphysik/Festkörperphysik, Ruhr-Universität Bochum, 44780 Bochum, Germany and*

⁴ PIMM, ENSAM, 151 Boulevard de l'Hôpital, 75013 Paris, France

Co₂MnSi (CMS) films of different thicknesses (20, 50 and 100 nm) were grown by radio frequency (RF) sputtering on a-plane sapphire substrates. Our X-rays diffraction study shows that, in all the samples, the cubic $\langle 110 \rangle$ CSM axis is normal to the substrate and that there exist well defined preferential in-plane orientations. Static and dynamic magnetic properties were investigated using vibrating sample magnetometry (VSM) and micro-strip line ferromagnetic resonance (MS-FMR), respectively. From the resonance measurements versus the direction and the amplitude of an applied magnetic field we derive most of the magnetic parameters: magnetization, gyromagnetic factor, exchange stiffness coefficient and magnetic anisotropy terms. The in-plane anisotropy can be described as resulting from the superposition of two terms showing a two-fold and a four-fold symmetry without necessarily identical principal axes. The observed behavior of the hysteresis loops is in agreement with this complex form of the in-plane anisotropy

PACS numbers: 76.50.+g, 78.35.+c, 75.30.Gw, 75.40.Gb

Keywords: Heuslers, magnetic anisotropy, spin waves, FMR and half-metals.

I. INTRODUCTION

The strong spin polarization at the Fermi level of full Heusler alloys and their high Curie temperature make of them potential candidates for applications. Thus, these materials have been very recently inserted in spintronics devices films made of Co₂MnSi full Heusler, which has a Curie temperature of 985 K [1,2], in order to be used in magnetic tunnel junctions (MTJs) containing one or two Co₂MnSi electrodes and different barriers [3-8]. Heusler alloys were used as MTJ electrodes with an amorphous Al-oxide barrier [9-12] allowing for a tunnel magnetoresistance (TMR) ratio of 159% at 2 K in a Co₂MnSi/Al-O/CoFe structure [6]. A large TMR ratio, up to 753% at 2 K and of 217% at room temperature, was obtained with Co₂MnSi used in TMJs with MgO barriers [13].

Despite this intense research activity on Heusler alloys, which is mainly focused on the way to improve the tunnel magnetoresistance, the static and dynamic magnetic properties of such alloys remain less explored [14-17]. The dynamics of these materials within the 1-10 GHz frequency range, which determines the high-speed response, is a key for their future technologic applications, especially in view of increasing data rates in magnetic storage devices. Moreover, the exchange stiffness constant A_{ex} which describes the strength of the exchange interaction inside Co₂MnSi films is an important parameter from both fundamental and application points of view. Therefore, the aim of this paper is to investigate the static and dynamic magnetic properties of Co₂MnSi thin films and their relations with their structure.

The paper is organized as follows: in section II we briefly present the preparation of the samples and their structural properties investigated by X-rays diffraction (XRD). Section III exposes their main static magnetic characteristics derived from our vibrating sample magnetometry (VSM) measurements. Section IV presents and discusses our dynamic measurements performed with the help of micro-strip ferromagnetic resonance (MS-FMR). In section V, conclusions are drawn.

II. SAMPLE PREPARATION AND STRUCTURAL PROPERTIES

The Co₂MnSi thin films (20, 50 and 100 nm in thickness) were deposited on a-plane sapphire substrate by UHV-magnetron rf-sputtering using pure Ar at a pressure of 5×10^{-3} mbar as sputter gas. The base pressure of the sputtering system was 2×10^{-9} mbar, the sputtering rate was 0.03 nm.s^{-1} for Co₂MnSi and 0.025 nm.s^{-1} for the previously deposited vanadium seed underlayer. During the deposition the temperature of the substrates was kept constant at 470°C. Heusler alloy targets with a diameter of 10 cm were cut from single phase, stoichiometric ingots prepared by high frequency melting of the components in high purity graphite crucibles. The Al₂O₃ sapphire a-plane substrate was, as mentioned above, preliminarily covered with a 5 nm thick vanadium-seed-layer in order to induce a high quality (110) growth of the Heusler compound. After cooling them down to room temperature all the films were subsequently covered by a 5 nm thick gold layer protecting them against oxidation.

*electronic adress: belmeguenai.mohamed@univ-paris13.fr

XRD measurements were performed using a Four-

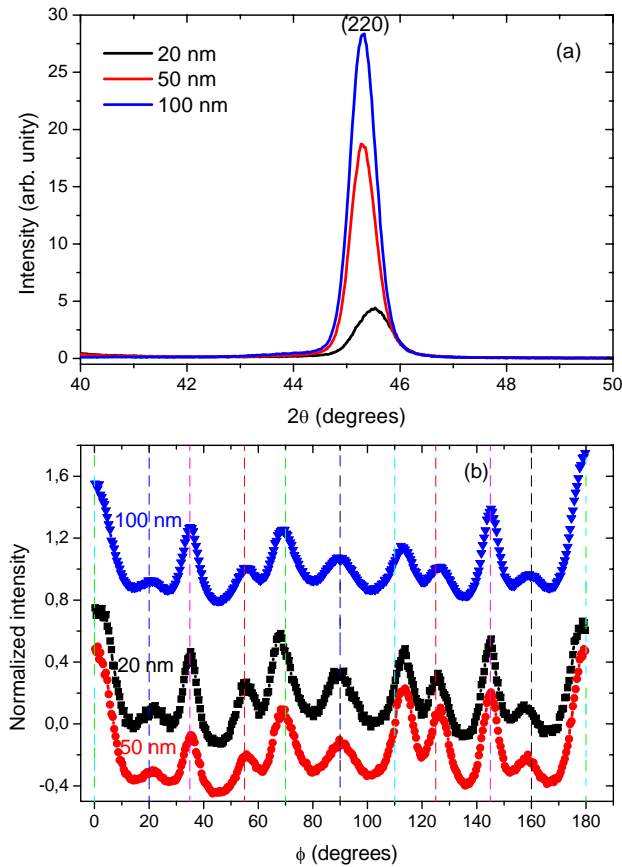


Figure 1: (Color online) (a) X-ray Bragg scan using the $\text{Cu K}\alpha_1$ radiation for the 100 nm thick Co_2MnSi thin film. (b) Angular variations of the intensity around 60° for different Co_2MnSi thin films. Graphs are shifted vertically with a respect to that of 20 nm thick samples for clearness. The vertical color and dashed lines refer to the expected positions of the diffraction peak relative to the different variants belonging to the observed 4 families.

Circle diffractometer in Bragg-Brentano geometry in order to obtain $\theta - 2\theta$ patterns and ϕ -scans, operating at 40 kV and 40 mA, and using a Cu X-rays source ($\lambda = 0.1518$ nm). In all the films, the $\theta - 2\theta$ pattern (Figure 1a) indicates that a $\langle 110 \rangle$ -type cubic axis is normal to the sample plane. The Co_2MnSi deduced cubic lattice constant (e.g.: $a = 5.658$ Å for the 100 nm thick sample) is in good agreement with the previously published value (5.654 Å) [2]. The samples behave as 110 fiber textures containing well defined zones showing significantly higher intensities, as shown in Figure 1b, which represents ϕ -scans at $\psi = 60^\circ$ (here, ψ is the declination angle between the scattering vector q and the direction normal to the film, ϕ is the rotational angle around this direction). The regions related to the observed maxima correspond to orientation variants which can be grouped into four families. Two of them were observed in a previous study [18, 19] concerning thin films of a neighboring

Heusler compound, Co_2MnGe , prepared using an identical protocol: in the first one the threefold axis is oriented along the c rhombohedral direction of the sapphire substrate, thus defining two kinds of distinct domains respectively characterized by their $[001]$ axis inclined at $+54.5^\circ$ or at -54.5° with respect to this c orientation. The second family is rotated by 90° from the first one and also contains two variants. In addition, we observe a third family consisting in domains with their $[001]$ axis along c and a fourth one with their $[001]$ axis normal to c . This distribution into 6 kinds of domains does not appreciably vary from sample to sample, as shown on Figure 1b. This difference in the structure between the Co_2MnSi and Co_2MnGe films probably arises from the variation of the lattice mismatch.

III. MAGNETIC PROPERTIES

A. Static magnetic measurements

For all the samples the hysteresis curves were studied at room temperature with an in-plane magnetic field H applied along various orientations, as shown in Figure 2 (φ_H is the angle between H and the c -axis of the substrate). The variations of the reduced remanent magnetization (M_r/M_s) as function of φ_H are also depicted in Figure 4, in view of comparison with other results discussed in the next section. For any given direction of the applied field the shape of the hysteresis loop is sample dependent, suggesting significant differences in the amplitudes and in the principal directions describing the in-plane anisotropy. Let us briefly discuss the case of the 50 nm film: as shown on Figure 2b, when H lies along c ($\varphi_H = 0^\circ$) a typical easy axis square-shaped loop is observed, with a full normalized remanence ($M_r/M_s = 0.99$) and a coercive field of 20 Oe. As φ_H increases M_r/M_s decreases and the hysteresis curve tends to transform into a hard axis loop. When φ_H reaches 70° its shape becomes more complicated: it consists into three smaller loops. A further increase of jH restores an almost rectangular shape. Notice the observed difference between orthogonal directions ($\varphi_H = 45^\circ$ vs $\varphi_H = 135^\circ$ or: $\varphi_H = -45^\circ$ vs $\varphi_H = -135^\circ$) which prevents a simple interpretation based on a four-fold in-plane anisotropy. Our data qualitatively agree with a description of the in-plane anisotropy in terms of an addition of four-fold and two-fold contributions with slightly misaligned easy axes.

Figures 2a and 2c show a series of hysteresis loops related to the other films: here again, they qualitatively agree with the above description, but with different relative contributions and orientations of the two-fold and of the four-fold anisotropy terms. At evidence, a quantitative estimation of the pertinent in-plane anisotropy terms monitoring the dynamic properties presented in the next section cannot be derived assuming hysteresis behaviour based on the coherent rotation model. However, as dis-

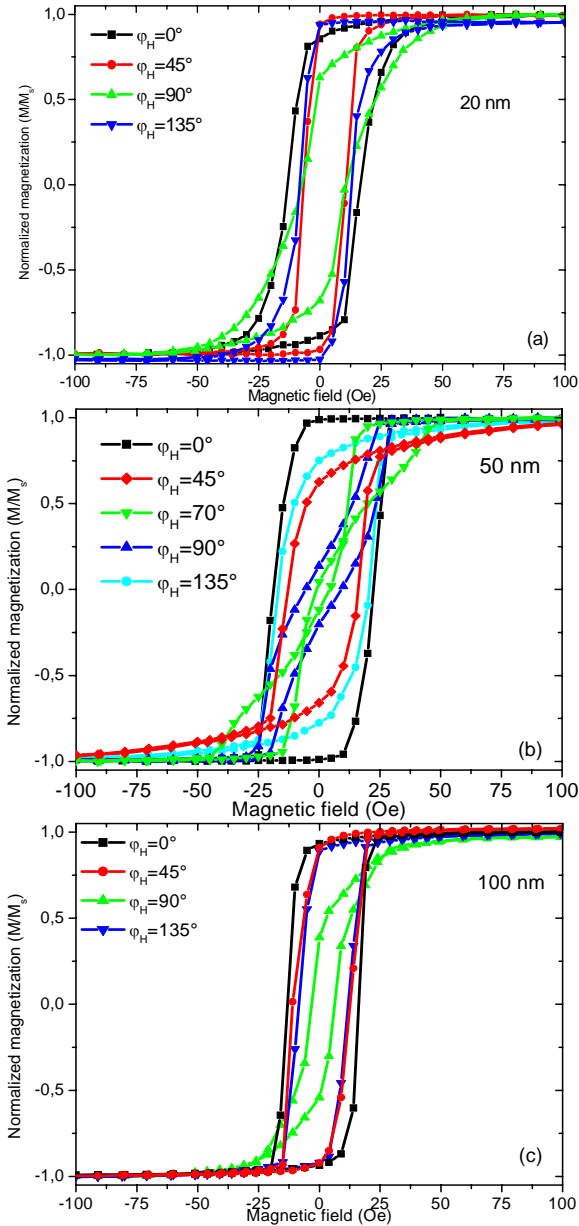


Figure 2: (Color online) VSM magnetization loops of the (a) 20 nm thick, (b) 50 nm thick and (c) 100 nm thick Co_2MnSi samples. The magnetic field is applied parallel to the film surface, at various angles (φ_H) with the c -axis of the sapphire substrate.

cussed in the following, this model provides a satisfactory account of the angular variation of M_r/M_s .

B. Dynamic magnetic properties

The dynamic magnetic properties were scrutinized using with the help of a previously described MS-FMR [18, 19] setup. The resonance frequencies are obtained from a fit assuming a lorentzian derivative shape of the

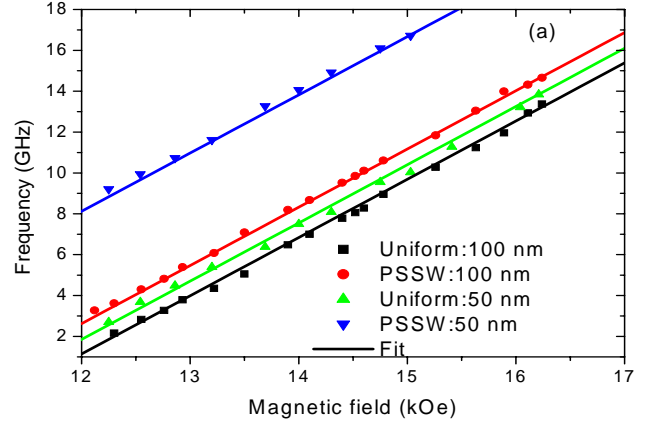


Figure 3: (Color online) Field-dependence of the resonance frequency of the uniform precession and of the first perpendicular standing spin wave excited (PSSW) mode of 50 nm and 100 nm thick films. The magnetic field is applied perpendicular to the film plane. The fits are obtained using equation (3) with the parameters indicated in the Table I.

recorded spectra. As in ref. [18], we assume a magnetic energy density which, in addition to Zeeman, demagnetizing and exchange terms, is characterized by the following anisotropy contribution:

$$E_{anis.} = K_{\perp} \sin^2 \theta_M - \frac{1}{2}(1 + \cos(2(\varphi_M - \varphi_u)))K_u \sin^2 \theta_M - \frac{1}{8}(3 + \cos 4(\varphi_M - \varphi_4))K_4 \sin^4 \theta_M \quad (1)$$

In the above expression, θ_M and φ_M respectively represent the out-of-plane and the in-plane (referring to the c -axis of the substrate) angles defining the direction of the magnetization M_s ; φ_u and φ_4 stand for the angles of the uniaxial axis and of the easy fourfold axis, respectively, with this c -axis. With these definitions K_u and K_4 are necessarily positive. As in ref. [18], it is convenient to introduce the effective magnetization $4\pi M_{eff} = 4\pi M_s - 2K_{\perp}/M_s$, the uniaxial in-plane anisotropy field $H_u = 2K_u/M_s$ and the fourfold in-plane anisotropy field $H_4 = 4K_4/M_s$.

For an in-plane applied magnetic field H , the studied model provides the following expression of the frequencies of the experimentally observable magnetic modes:

$$F_n^2 = \left(\frac{\gamma}{2\pi}\right)^2 \left(H \cos(\varphi_H - \varphi_M) + \frac{H_4}{2} \cos 4(\varphi_M - \varphi_4) + H_u \cos 2(\varphi_M - \varphi_u) + \frac{2A_{ex.}}{M_s} \left(\frac{n\pi}{d}\right)^2 \right) \times \left(H \cos(\varphi_H - \varphi_M) + 4\pi M_{eff} + \frac{H_4}{2} (3 + \cos 4(\varphi_M - \varphi_4)) + \frac{H_u}{2} (1 + \cos 2(\varphi_M - \varphi_u)) + \frac{2A_{ex.}}{M_s} \left(\frac{n\pi}{d}\right)^2 \right) \quad (2)$$

For H normal to the sample plane, large magnetic fields are applied (enough to allow for $M_s \parallel H$) and thus the magnetic in-plane anisotropies can be neglected. Therefore, the frequency linearly varies versus H as:

$$F_{\perp} = \frac{\gamma}{2\pi} \left(H - 4\pi M_{eff} + \frac{2A_{ex.}}{M_s} \left(\frac{n\pi}{d}\right)^2 \right) \quad (3)$$

d (nm)	D ($\mu\text{erg.cm}^{-1}$)	$4\pi M_{eff}$ (kOe)	H_u (Oe)	H_4 (Oe)	φ_u (deg.)	φ_4 (deg.)
20		11	20	72	0	45
50	2.87	11.35	26	88	-13	0
100	2.56	11.6	16	48	0	45

Table I: Magnetic parameters obtained from the best fits to our experimental results. φ_u and φ_4 are the angles of the in-plane uniaxial and of the four-fold anisotropy easy axes, respectively.

In the above expressions the gyromagnetic factor γ is related to the effective Lande factor g through: $(\gamma/2\pi) = g \times 1.397 \times 10^6 \text{ s}^{-1} \cdot \text{Oe}^{-1}$. The uniform mode corresponds to $n = 0$. The other modes to be considered (perpendicular standing spin waves: PSSW) are connected to integer values of n : their frequencies depend upon the exchange stiffness constant A_{ex} and upon the film thickness d .

For all the films the magnetic parameters at room temperature were derived from MS-FMR measurements.

1. Gyromagnetic g -factor and spin wave stiffness

In perpendicular configuration the MS-FMR technique allows for deriving the values of g and of $4\pi M_{eff}$ from the variation of the resonance frequency versus the magnitude of the applied field using equation (3). The MS-FMR field-dependences of the resonance frequencies of the uniform and of the PSSW modes are shown on Figure 3 for the 50 nm and the 100 nm thick samples. The frequencies vary linearly with H . The PSSW mode shows a frequency higher than the uniform one, by an amount independent of H , as expected from the studied model. The derived value of g is independent of the sample: $g = 2.04$. It is in good agreement with previous determinations [15]. The effective demagnetizing field $4\pi M_{eff}$ slightly increases versus the sample thickness but remains close to the saturation magnetization (12200 Oe) given by Hamrle et al. [20]: it is reported in Table I. The best fits for the observed PSSW are obtained using $A_{ex} = 2.87 \times 10^{-6} \text{ erg.cm}^{-1}$ and $A_{ex} = 2.56 \times 10^{-6} \text{ erg.cm}^{-1}$ for the 50 nm and the 100 nm thick films respectively, in good agreement with the result published by Hamrle et al. ($A_{ex} = 2.35 \times 10^{-6} \text{ erg.cm}^{-1}$) [20].

2. In-plane anisotropies

Figures 4b, 4d and 4f illustrate the experimental in-plane angular dependence of the frequency of the uniform mode in the 20, 50 and 100 nm thick films, compared to the obtained fits using equation (2). For all the samples, the obtained values of the magnetic parameters corresponding to the best fits are reported in Table I.

In all the investigated films the c -axis of the substrate

coincides with a principal direction of the four-fold magnetic anisotropy: it defines a hard axis ($\varphi_4 = 45^\circ$) except, surprisingly, in the 50 nm sample for which it defines an easy axis ($\varphi_4 = 0^\circ$). The directions of the principal axes of the two-fold anisotropy are sample dependent. The observed variations of the in-plane magnetic anisotropy are not clearly related either to the thickness or to the crystallographic texture (which does not significantly change). During the preparation of the films uncontrolled parameters presumably induce different stress conditions giving rise to changes in the magnetic anisotropy. Finally, it is interesting to notice that the set of in-plane magnetic anisotropy parameters deduced from the in-plane angular dependence of the magnetic resonance for the 20 nm, 50 nm and 100 nm thick samples allows for a good fit of the angular variation of the normalized static remanence calculated with the help of the coherent rotation model, as shown in Figures 4. This variation only depends on φ_u , φ_4 and H_u/H_4 .

It results from the present study and from our previous ones [18, 19] that the growth of Heusler thin films on sapphire substrates is complex and depends on the conditions of the sample preparation. Therefore the magnetic properties cannot be tuned rigorously.

IV. CONCLUSION

Co_2MnSi films of thicknesses varying from 20, 50 and 100 nm were prepared by sputtering on a a -plane sapphire substrate. They show practically identical crystallographic textures, as revealed by our X-rays diffraction studies, with a cubic [110] axis normal to the film plane and with a well defined manifold of in-plane orientations referring to the c -axis of the substrate. The micro-strip ferromagnetic resonance gives access to effective g factors which do not differ from each other and to effective demagnetizing fields which are close to the magnetization at saturation and which slightly increase with the sample thickness. In addition, this technique allowed us for evaluating the exchange stiffness constant which, as expected, was found not to significantly depend on the studied sample. The in-plane anisotropy was investigated through the study of the dependence of the resonance frequency versus the orientation of an in-plane applied magnetic field: it presents two contributions, showing a

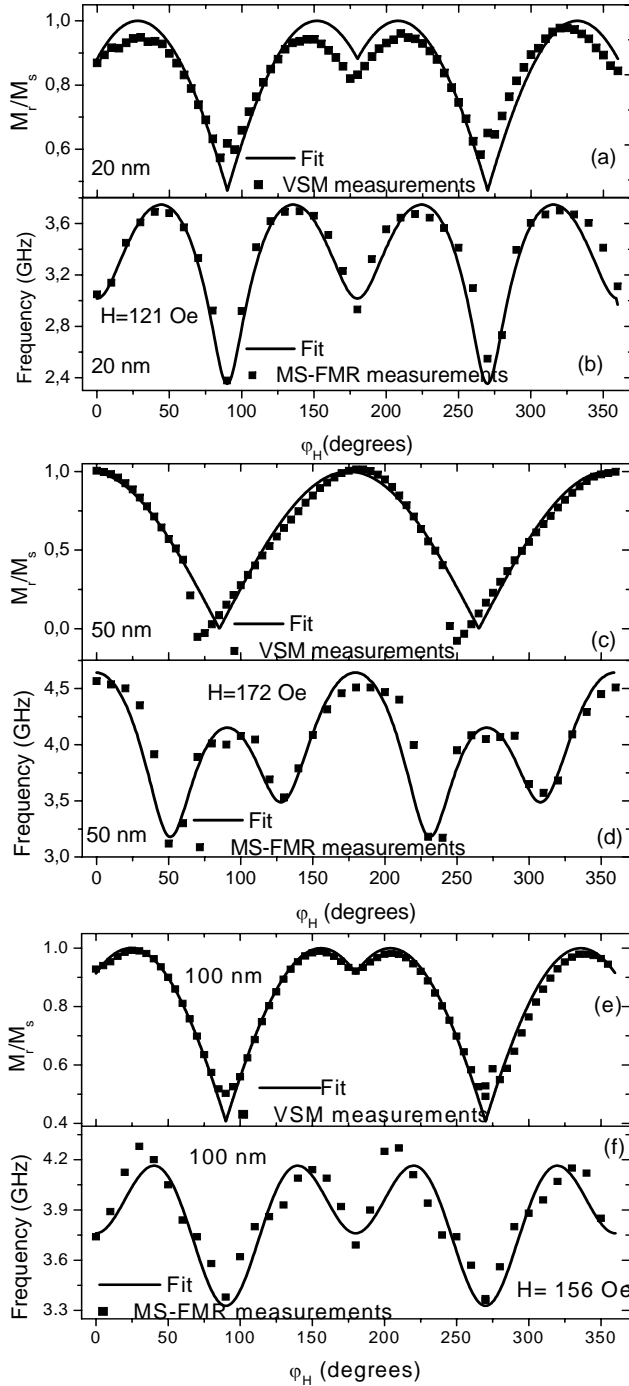


Figure 4: Reduced remanent magnetization of the (a) 20 nm, of the (c) 50 nm and of (e) 100 nm thick Co_2MnSi films. The full lines are obtained from the energy minimization using the parameters reported in Table I. (b), (d) and (f) show the compared in-plane angular-dependences of the resonance frequency of the uniform modes. The fit is obtained using equation (2) with the parameters indicated in Table I.

four-fold and a two-fold axial symmetry, respectively. A principal four-fold axis parallel to c is always found, but it can be the easy or the hard axis. Depending on the studied film the two-fold axes can be misaligned with the four-fold ones. The angular dependence of the remanent normalized magnetization, studied by VSM and analyzed within the frame of a coherent rotation model, is in agreement with these conclusions. The general magnetic behavior is similar to the previously published one observed in Heusler Co_2MnGe films [18, 19]. Apparently, there is no simple relation between the observed dispersion of the in-plane anisotropy parameters and the thickness or the crystallographic texture of the samples.

- Tanaka, J. Nowak, J. S. Moodera, A. Barry, and J. M. D. Coey, *Science* 282, 85 (1998).
- [2] [2] P. J. Webster, *J. Phys. Chem. Solids* 32, 1221 (1971)
- [3] [3] J. Schmalhorst, S. Kämmerer, M. Sacher, G. Reiss, A. Hütten, and A. Scholl, *Phys. Rev. B* 70, 024426 (2004).
- [4] [4] Y. Sakuraba, J. Nakata, M. Oogane, H. Kubota, Y. Ando, A. Sakuma, and T. Miyazaki, *Japan J. Appl. Phys.* 44, L1100 (2005).
- [5] [5] M. Oogane, Y. Sakuraba, J. Nakata, H. Kubota, Y. Ando, A. Sakuma, and T. Miyazaki, *J. Phys. D: Appl. Phys.* 39, 834 (2006).
- [6] [6] Y. Sakuraba, M. Hattori, M. Oogane, Y. Ando, H. Kato, A. Sakuma, T. Miyazaki, and H. Kubota, *Appl. Phys. Lett.* 88, 192508 (2006).
- [7] [7] K. Inomata, N. Ikeda, N. Tezuka, R. Goto, S. Sugimoto, M. Wojcik, and E. Jedryka, *Sci. Technol. Adv. Mat.* 9, 014101 (2008).
- [8] [8] T. Ishikawa, S. Hakamata, K. Matsuda, T. Uemura, and M. Yamamoto, *J. Appl. Phys.* 103, 07A919 (2008).
- [9] [9] C. T. Tanaka, J. Nowak and J. S. Moodera, *J. Appl. Phys.* 86, 6239 (1999)
- [10] [10] S. Kämmerer, A. Thomas, A. Hütten and G. Reiss, *Appl. Phys. Lett.* 85, 79 (2004)
- [11] [11] A. Conca, S. Falk, G. Jakob, M. Jourdan and H. Adrian, *J. Magn. Magn. Mater.* 290–291, 1127 (2004)
- [12] [12] H. Kubota, J. Nakata, M. Oogane, Y. Ando, A. Sakuma and T. Miyazaki, *Japan. J. Appl. Phys.* 43 L984 (2004)
- [13] [13] S. Tsunegi, Y. Sakuraba, M. Oogane, K. Takanashi, Y. Ando, *Appl. Phys. Lett.* 93, 112506 (2008).
- [14] [14] Y. Liu, L. R. Shelford, V. V. Kruglyak, R. J. Hicken, Y. Sakuraba, M. Oogane, and Y. Ando, *Phys. Rev. B* 81, 094402 (2010)
- [15] [15] B. Rameev, F. Yildiz, S. Kazan, B. Aktas, A. Gupta, L. R. Tagirov, D. Rata, D. Buerger, P. Gruenberg, C. M. Schneider, S. Kämmerer, G. Reiss, and A. Hütten, *phys. stat. sol. (a)* 203, 1503 (2006)
- [16] [16] R. Yilgin, M. Oogane, Y. Ando, T. Miyazaki, *J. Mag. Mag. Mat.* 310, 2322 (2007)
- [17] [17] O. Gaier, J. Hamrle, S. J. Hermsdoerfer, H. Schultheiß, B. Hillebrands, Y. Sakuraba, M. Oogane, and Y. Ando, *J. Phys. D: Appl. Phys.* 43 (2010) 193001
- [18] [18] M. Belmeguenai, F. Zighem, Y. Roussigné, S-M. Chérif, P. Moch, K. Westerholt, G. Woltersdorf, and G. Bayreuther *Phys. Rev. B* 79, 024419 (2009).
- [19] [19] M. Belmeguenai, F. Zighem, T. Chauveau, D. Faurie, Y. Roussigné, S-M. Chérif, P. Moch, K. Westerholt and P. Monod, *J. Appl. Phys.* 108, 063926 (2010)
- [20] [20] J. Hamrle, O. Gaier, Seong-Gi Min, B. Hillebrands, Y. Sakuraba and Y. Ando, *J. Phys. D: Appl. Phys.* 42, 084005 (2009)